Block encoding of sparse matrices with a periodic diagonal structure

Zecchi, A. A.; Sanavio, C.; Cappelli, L.; Perotto, S.; Roggero, A.; Succi, S.

Block encoding of sparse matrices with a periodic diagonal structure

Alessandro Andrea Zecchi[1], Claudio Sanavio[2], Luca Cappelli[3], Simona Perotto[1], Alessandro Roggero[4,5] and Sauro Succi[2]

February 13, 2026

[1]MOX - Dipartimento di Matematica
Politecnico di Milano
Piazza L. da Vinci, 32, I-20133 Milano, Italy
alessandroandrea.zecchi@polimi.it

[2]Fondazione Istituto Italiano di Tecnologia,
Center for Life Nano-Neuroscience at la Sapienza,
Viale Regina Elena 291, 00161 Roma, Italy

[3] Dipartimento di Fisica dell'Università di Trieste,
Via Tiepolo 11, 34131 Trieste, Italy

[4] Physics Department, University of Trento,
Via Sommarive 14, 38123 Trento, Italy

[5] INFN-TIFPA Trento Institute of Fundamental Physics and Applications,
Via Sommarive 14, 38123 Trento, Italy

Abstract

Block encoding is a successful technique used in several powerful quantum algorithms. In this work we provide an explicit quantum circuit for block encoding a sparse matrix with a periodic diagonal structure. The proposed methodology is based on the linear combination of unitaries (LCU) framework and on an efficient unitary operator used to project the complex exponential at a frequency ω multiplied by the computational basis into its real and imaginary components. We demonstrate a distinct computational advantage with a $O(\mathrm{poly}(n))$ gate complexity, where n is the number of qubits, in the worst-case scenario used for banded matrices, and $O(n)$ when dealing with a simple diagonal matrix, compared to the exponential scaling of general-purpose methods for dense matrices. Various applications for the presented methodology are discussed in the context of solving differential problems such as the advection-diffusion-reaction (ADR) dynamics, using quantum algorithms with optimal scaling, e.g., quantum singular value transformation (QSVT). Numerical results are used to validate the analytical formulation.

1

1 Introduction

The quantum computing paradigm harnesses the features of quantum mechanics to perform computations [1] and is rapidly advancing toward practical applications in many research areas. Several quantum algorithms, including recent innovative developments, outperform conventional classical methods and offer significant speedup for various problems [2, 3]. Moreover, many important quantum algorithms share ideas and techniques that are typically used as subroutines to perform a specific task. For instance, the quantum Fourier transform is used for both the Shor's algorithm, which aims at finding the prime factors of an integer, and the Harrow–Hassidim–Lloyd algorithm, the latter used for finding the solution of a linear system [4].

A powerful subroutine known as block encoding emerged in the context of Hamiltonian simulation through qubitization [5]. Block encoding enables numerous complex matrix operations on quantum computers and has become a fundamental tool in developing new algorithms. This technique is widely used in quantum applications for chemistry, linear algebra, optimization, and simulating physical systems, and can be used to encode a possibly non-unitary matrix as a sub-block of a larger unitary operator [6, 7, 8]. Here we briefly recall the main mathematical aspects. Given a matrix $A \in \mathbb{C}^{2^n \times 2^n}$ we define the unitary matrix $U_A \in \mathbb{C}^{2^{n+m} \times 2^{n+m}}$ that provide a block encoding of A with m ancillary qubits, as

$$U_A = \begin{bmatrix} A/\alpha & * \\ * & * \end{bmatrix}. \tag{1}$$

The elements $*$ guarantee the unitarity of U_A while the scaling factor α, also called subnormalization, ensures that $\|A/\alpha\| \leq 1$ [9] where $\|\cdot\|$ is the usual spectral matrix norm. Therefore, the scaling factor must satisfy the following inequality $\alpha \geq \|A\|$, but usually a lower scaling is favorable since the efficiency of many quantum algorithms improves as α reduces. Finding a block encoding scheme with $\alpha = \|A\|$ for a generic matrix A remains an open problem.

Recognizing the significance of block encoding has motivated extensive research on optimizing its construction for various classes of matrices [10, 11, 12]. For dense matrices, i.e., with almost all elements different from zero, typically occurring when loading classical data, there has been extensive research [11] also regarding the quantum random access memory query model [13]. A method, named FABLE, to generate fast approximate quantum circuits for dense matrices was proposed by [14] and subsequently extended for unstructured sparse matrices [15]. Block encoding can be also used for ladder operators acting on fermionic and bosonic modes, and can be a powerful tool for simulating quantum field theories [16].

However, currently available methods for block encoding sparse matrices often lack the ability to efficiently exploit specific structural regularities [9]. These patterns arise frequently in engineering applications, for instance, when modeling second-order elliptic differential problems with periodic coefficients.

In this work we introduce a new block encoding method based on the LCU framework for sparse matrices with a periodic structure. In particular, we focus on sparse

banded matrices and provide an explicit quantum circuit that can be easily extended to any periodic signal with a given number of frequency components. This method effectively exploits the periodicity of the matrices improving efficiency with respect to known methods and it is based on a specific unitary based on the complex exponential at a particular frequency which can be easily linked to sinusoidal functions representing its real and imaginary part. In Section 2 the proposed methodology is presented and characterized for a single frequency while the extension to sparse banded matrices is considered in Section 3 along with the case with a more general periodic structure decomposed into different frequencies. Various applications are analyzed in Section 4 in the context of solving an elliptic partial differential equation (PDE) problem on a quantum computer. A paradigmatic example is provided by the classical dynamical behavior of ADR differential equation with periodically varying coefficients. The numerical results are presented in Section 5. Finally, we discuss the outlooks and conclusions of our work in Section 6.

2 Quantum circuit

In this section, we describe the general idea behind our framework and provide a detailed analysis of the quantum circuit for block encoding sparse matrices with a periodic structure on the main diagonal. We follow standard conventions used in the quantum computing literature, writing quantum states in the Dirac notation $|\cdot\rangle$ and using standard quantum gates. For the binary representation of an integer $k \in \mathbb{N}$ we employ the little-endian convention with $k = k_{n-1} \cdot 2^{n-1} + \cdots + k_1 \cdot 2^1 + k_0 \cdot 2^0$ and where k_0 denotes the least significant bit. The qubit associated to the least significant bit appears at the bottom in quantum circuit diagrams.

2.1 Diagonal sinusoidal matrix

We start by considering two diagonal matrices $C(\omega, \phi), S(\omega, \phi) \in \mathbb{R}^{N \times N}$, where $N = 2^n$ with n being the number of working qubits, characterized by oscillating components with frequency $\omega \in \mathbb{R}$, such that:

$$C(\omega, \phi)_{ij} = \cos((i-1)\omega + \phi)\delta_{ij} \tag{2}$$

$$S(\omega, \phi)_{ij} = \sin((i-1)\omega + \phi)\delta_{ij}, \tag{3}$$

where δ_{ij} is the Kronecker delta function for the matrix indices $i, j = 1, \ldots, N$ and $\phi \in \mathbb{R}$ is a phase term. We consider ω taking values in $[0, 2\pi)$ as it does not change the overall result. In our construction, we take advantage of the fact that these two matrices are the real and imaginary components of a diagonal unitary operator such that $(C(\omega, \phi) + \mathrm{i}S(\omega, \phi))_{ij} = e^{\mathrm{i}((i-1)\omega + \phi)}\delta_{ij} = V(\omega, \phi)$ with i being the imaginary unit. In particular, this operator can be written as

$$V(\omega, \phi) = e^{\mathrm{i}\phi}\mathrm{diag}\left(1, e^{\mathrm{i}\omega}, e^{\mathrm{i}2\omega}, e^{\mathrm{i}3\omega}, \ldots, e^{\mathrm{i}(N-1)\omega}\right), \tag{4}$$

with ϕ being a global factor acting as a phase shift for the cosine and sine components. Without loss of generality, we set from now on $\phi = 0$, thus writing in V, C and S only the dependence on ω. The unitary operator $V(\omega)$ acts on the computational basis state $|k\rangle$ as

$$V(\omega)|k\rangle = e^{i\omega k}|k\rangle, \tag{5}$$

where k can be expanded in binary as $k = \sum_{q=0}^{n-1} k_q 2^q$ with $k_q \in \{0, 1\}$. Substituting this expression of k into (5) we can write that

$$e^{i\omega k} = e^{i\omega \sum_{q=0}^{n-1} k_q 2^q} = \prod_{q=0}^{n-1} e^{i\omega k_q 2^q}, \tag{6}$$

and since the term has been factored into a product over bits, the unitary operator V can be implemented as a sequence of single-qubit rotations about the Z axis, i.e., of phase gates

$$V(\omega) = \prod_{q=0}^{n-1} P(2^q \omega), \tag{7}$$

using the definition $P(\theta) = \mathrm{diag}(1, e^{i\theta})$. The corresponding circuit is depicted in Figure 1, and requires a number of single qubit phase gates equal to the number of qubits and, therefore, it can be regarded as highly efficient and attainable on a near term quantum device. Clearly, if a phase angle θ is sufficiently small, the gate's effect on the quantum state becomes negligible, allowing it to be discarded during circuit optimization [17, 18]. Hence, in some cases, many phase gates can be removed without significantly affecting the result, further reducing the computational cost of the operator. For instance, for small frequencies $\omega \le 2\pi/N$, we can approximate the unitary $V(\omega)$ with error at most ϵ rotating only the leading $\mathcal{O}(\log(1/\epsilon))$ qubits. This type of diagonal operator has already been studied for the Generalized Quantum Signal Processing (GQSP) framework to synthesize diagonal matrices using a Fourier decomposition into polynomials of $V(\omega)$ [19]. In that case, the operator was designed only for powers of the primitive N-th root of unity, i.e., $e^{ip\frac{2\pi}{N}}$ with p being an integer, to implement convolution operators in the quantum Fourier basis. Conversely, in our case the focus is on building a block encoding of a periodic real matrix, extending subsequently the result to a linear combination of operators with different, and arbitrary, frequencies.

The interference produced by the Hadamard gates allows us to isolate the real and imaginary components of the unitary $V(\omega)$. This construction leads to the following result.

Theorem 1 *Let $\omega \in \mathbb{R}$ and let $V(\omega) = V(\omega, 0)$ be the diagonal unitary operator defined in Equation (4). The unitary $U_{C(\omega)}$ acting on $n + 1$ qubits, defined as*

$$U_{C(\omega)} = (H \otimes I)(I \otimes V(\omega)^\dagger)(|0\rangle\langle 0| \otimes V(2\omega) + |1\rangle\langle 1| \otimes I)(H \otimes I), \tag{8}$$
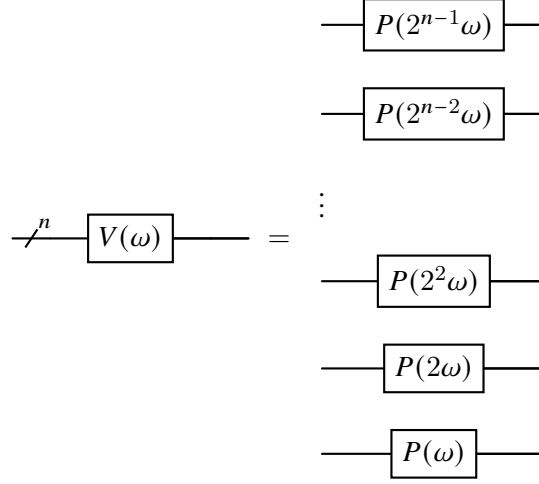
4

Figure 1: Quantum circuit to implement the diagonal unitary operator (4) using n phase gates.

is an exact block encoding of the diagonal matrix $C(\omega) = C(\omega, 0)$ defined in Equation (2) with sub-normalization factor $\alpha = 1$ and $m = 1$ ancilla qubit.

The proof follows from the direct application of the unitary operators and the identity $V(\omega)^\dagger = V(-\omega)$. If we consider an ancilla qubit initialized in $|0\rangle$ with a working register of size n having an arbitrary initial state $|\psi\rangle$, as depicted in Figure 2, the resulting overall state corresponds to the superposition

$$|\Psi_1\rangle = |0\rangle C(\omega)|\psi\rangle + \mathrm{i}|1\rangle S(\omega)|\psi\rangle. \tag{9}$$

The state $|\Psi_1\rangle$, depending on the result of the measurement performed on the ancilla qubit, collapses into either the state $C(\omega)|\psi\rangle$ or the state $S(\omega)|\psi\rangle$ on the working qubits up to a global phase.
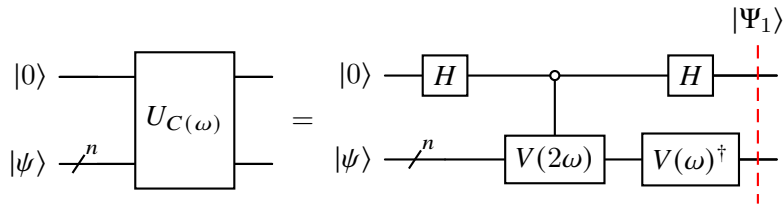

Figure 2: Block encoding circuit of the diagonal matrix C defined in Equation (2).

We remark that by recovering the dependency on the phase factor ϕ it is possible to retrieve the more general expressions of Equations (2) and (3). In addition, it is sufficient to add a Pauli-Y gate to the ancilla qubit to obtain

$$(Y \otimes I)|\Psi_1\rangle = Y(|0\rangle C(\omega)|\psi\rangle + \mathrm{i}|1\rangle S(\omega)|\psi\rangle) = |0\rangle S(\omega)|\psi\rangle + \mathrm{i}|1\rangle C(\omega)|\psi\rangle, \tag{10}$$

5

thus achieving a block encoding of the *sine* matrix $S(\omega)$ associated with the $|0\rangle$ state of the ancilla qubit.

The probability of the two outcomes of Equation (9) depends on the initial state $|\psi\rangle$. If we write the state as $|\psi\rangle = \sum_{k=0}^{N-1} c_k |k\rangle$, with $\sum_{k=0}^{N-1} |c_k|^2 = 1$, then the probability of measuring the state $|0\rangle$ is $p_0 = \sum_{k=0}^{N-1} |c_k|^2 \cos^2(k\omega)$, while the probability of measuring $|1\rangle$ is $p_1 = 1 - p_0 = \sum_{k=0}^{N-1} |c_k|^2 \sin^2(k\omega)$.

Employing the trigonometric identity $\cos(x)^2 = 1/2(1 + \cos(2x))$ it is also possible to write $p_0 = 1/2 + 1/2 \sum_{k=0}^{N-1} |c_k|^2 \cos(2k\omega)$ which shows that the probability oscillates around an *average* value of $1/2$ and depends both on the initial coefficients c_k and on the frequency ω. The probability p_0 is shown in Figure 3 for an initial uniform distribution (or superposition) with all equal coefficients, while for a single computational basis state k it oscillates exactly as $p_0 = \cos(k\omega)^2$. Instead, for a generic distribution the probability oscillates between 0 and 1 with an interference-like pattern.
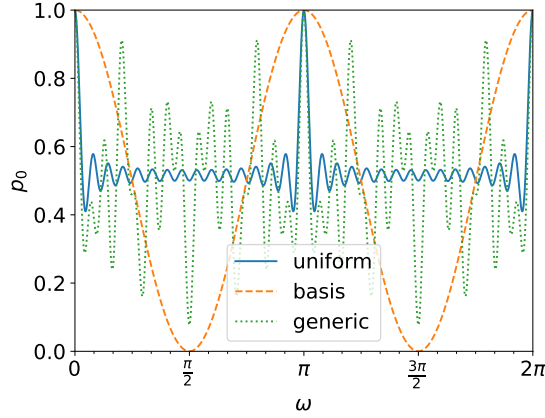

Figure 3: Probability p_0 of successfully applying the proposed block encoding for different values of ω and different choices of the initial state ψ, the uniform distribution (solid), the computational basis case (dashed) and a generic distribution (dotted). The quantum register of ψ consists of 4 qubits.

We point out that the proposed circuit for block encoding a diagonal non unitary matrix (see Figure 2) has the advantage of requiring less controlled multi-qubit operations with respect to other schemes designed for more general matrices[20]. The circuit in Figure 2 can be implemented straightforwardly using $3n$ phase gates and $2n$ CNOT gates [21]. An even simpler implementation requiring only n phase gates instead can be obtained using the implementation shown in Figure 4.
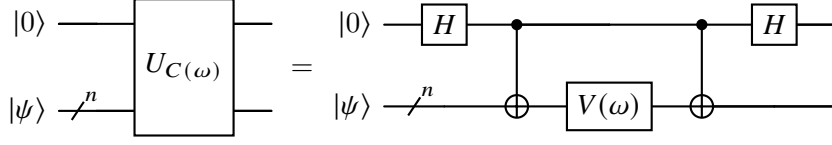
6

Figure 4: Alternative block encoding circuit of the diagonal matrix C defined in Equation (2). The CNOT gates have one control and n targets.

2.2   Shift permutation matrices

The left L and right R shift permutation matrices are defined as follows

$$
L = \begin{bmatrix} 0 & 0 & \cdots & \cdots & 1 \\ 1 & 0 & 0 & \cdots & 0 \\ \vdots & 1 & \ddots & \ddots & \vdots \\ \vdots & \ddots & \ddots & \ddots & \vdots \\ 0 & 0 & \cdots & 1 & 0 \end{bmatrix}, \quad R = \begin{bmatrix} 0 & 1 & \cdots & \cdots & 0 \\ 0 & 0 & 1 & \ddots & 0 \\ \vdots & 0 & \ddots & \ddots & \vdots \\ \vdots & \vdots & \ddots & \ddots & 1 \\ 1 & 0 & \cdots & \cdots & 0 \end{bmatrix}.
\tag{11}
$$

These operators correspond to the addition and subtraction arithmetic operations modulo N and can be used to apply a shift to a diagonal matrix. The shift operators can be constructed in a straightforward way following the circuit in Figure 5 using a sequence of multi-qubit controlled Toffoli gates. In this case the depth is quadratic in n and the number of Toffoli gates scales as $O(n^2)$, using a single *dirty* (without requiring re-initialization) ancilla qubit [22]. Further savings can be achieved using the approach applied to the quantum adder in [23] which requires $n-1$ clean ancilla qubits but has a Toffoli cost of only $O(n)$.

By iteratively applying s times one of these operators, i.e., R^s or L^s, further shifts to right or the left, respectively, can be achieved, while appending one of these operators to the working register of the circuit defined in Figure 2 is an effective strategy to shift the periodic structures of Equations (2) and (3). For instance, the result of applying the right shift operator to the matrix $C(\omega)$ is

$$
RC(\omega) = \begin{bmatrix} 0 & \cos(\omega) & \cdots & \cdots & 0 \\ 0 & 0 & \cos(2\omega) & \ddots & 0 \\ \vdots & 0 & \ddots & \ddots & \vdots \\ \vdots & \vdots & \ddots & \ddots & \cos((N-1)\omega) \\ 1 & 0 & \cdots & \cdots & 0 \end{bmatrix}.
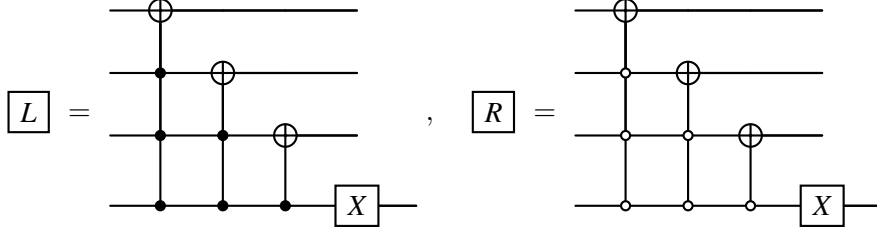\tag{12}
$$

Figure 5: Shift circuits for a quantum register of size 4.

3 Block encoding of sparse matrices with a periodic structure

We consider a sparse banded matrix $M \in \mathbb{R}^{N \times N}$, again with $N = 2^n$, whose off-diagonal configuration is Toeplitz with wrap-around and with an arbitrary structure on the main diagonal, namely

$$
M = \begin{bmatrix}
m_{11} & \alpha_2 & 0 & \cdots & \alpha_1 \\
\alpha_1 & m_{22} & \ddots & \ddots & 0 \\
0 & \alpha_1 & \ddots & \alpha_2 & \vdots \\
\vdots & \ddots & \ddots & \ddots & \alpha_2 \\
\alpha_2 & 0 & \cdots & \alpha_1 & m_{NN}
\end{bmatrix}.
\tag{13}
$$

This kind of matrix can arise when dealing with a directed cyclic graph with different weights for each vertex, or when dealing with the algebraic form resulting from the finite discretizations of partial differential equations with periodic boundary conditions [24, 25].

It is well known that by using the Linear Combinations of Unitary operations (LCU) framework, originally developed in [26], it is possible to decompose any operator O into a sum of J unitary matrices U_j, each one weighted by a real positive coefficient α_j, for $j = 0, 1, \ldots, J-1$, as

$$
O = \sum_{j=0}^{J-1} \alpha_j U_j.
\tag{14}
$$

In particular, the linear combination is achieved using a unitary state preparation operator $PREP$, and its inverse $PREP^\dagger$. More precisely, we can define the state preparation operator, acting onto a data register of $\lceil \log_2(J) \rceil$ qubits as

$$
PREP \ket{0} = \sum_{j=0}^{J-1} \sqrt{\frac{\alpha_j}{\alpha}} \ket{j},
\tag{15}
$$

with $\alpha = \sum_{j=0}^{J-1} \alpha_j$ being a proper normalization coefficient. In order to obtain the full

operator O we also need a $SELECT$ unitary defined as

$$SELECT = \sum_{j=0}^{J-1} |j\rangle\langle j|\otimes U_j \,, \tag{16}$$

so that we can write a rescaled version of our operator as follows

$$\frac{O}{\alpha} = \langle 0|(PREP)^\dagger (SELECT)(PREP)|0\rangle \,. \tag{17}$$

If the matrix M has a periodic structure on the main diagonal, we can employ the matrix $C(\omega)$ defined in Equation (2), and the left and right shift permutation matrices, to construct the following LCU, involving four positive real coefficients

$$M = \alpha_0 C(\omega) + \alpha_1 L + \alpha_2 R + \alpha_3 I. \tag{18}$$

In this case the resulting matrix is defined as in Equation (13) but with diagonal entries given by

$$m_{ii} = \alpha_0 \cos((i-1)\omega + \phi) + \alpha_3, \quad i = 1, \dots, N. \tag{19}$$

The quantum circuit depicted in Figure 6, is a block encoding of M using three ancillary qubits: one for the block encoding of $C(\omega)$ (see Theorem 1), and two for encoding the LCU coefficients into an appropriate quantum state. Post-selecting the ancillary qubits in the state $|000\rangle$ implements the desired matrix transformation.
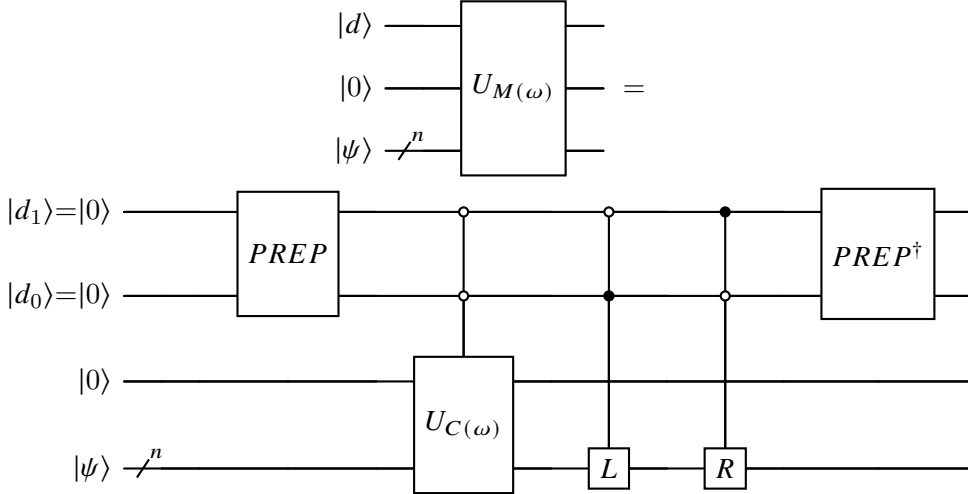

Figure 6: Block encoding of a sparse banded matrix with a periodic structure employing LCU.

This quantum circuit can be considered efficient as the gate complexity is $O(n^2)$ as seen from the analysis above where we have fully characterized its various components. The dominant cost is the implementation of the $SELECT$ circuit which requires J

multiply-controlled operations. The controlled version of $U_{C(\omega)}$ can be obtained by controlling the $V(\omega)$ unitary in Figure 4 from the two ancilla qubits. This can be done easily by adding two Toffoli with target an additional clean ancilla, n additional rotations and $2n$ CNOT gates controlled on the added ancilla. When using the unitary incrementer circuit from [23] to implement the shift operators L and R, their controlled version can be implemented using a constant number of additional gates. Finally, the Toffoli cost of implementing the sequence controls needed for the $SELECT$ operation can be brought down to only $O(J)$ using the unary iteration scheme proposed in [27], which organizes these controls into a ladder structure to optimize circuit depth. We also remark that for this block encoding scheme it is also possible to modify the quantum circuit to zero out the α_1 in the $(1, N)$-th entry of M and the α_2 in the $(N, 1)$-th entry of M, obtaining a tridiagonal matrix following the procedure explained in [9].

We provide for sake of concreteness a simple example with $n = 2$ working qubits, $\omega = \pi/2$ and using $PREP = H \otimes H$, therefore with $\alpha_j = 1/4, \quad \forall j$ for which the resulting matrix is simply given by

$$M = \frac{1}{4} \begin{bmatrix} \cos(0) + 1 & 1 & 0 & 1 \\ 1 & \cos(\pi/2) + 1 & 1 & 0 \\ 0 & 1 & \cos(\pi) + 1 & 1 \\ 1 & 0 & 1 & \cos(3\pi/2) + 1 \end{bmatrix}, \tag{20}$$

with the full circuit implementation given by Figure 6.

3.1 Fourier decomposition: periodic structure with more than one frequency

If we consider a generic signal it is possible to employ Fourier analysis to decompose it into its basic components. Employing this tool it is possible to express the original signal as a linear combination of periodic components at different frequencies. The same concept can be applied for the elements of a generic diagonal matrix. In particular, using the LCU framework it is also possible to extend the previous results to include matrices defined as in (13), that exhibit a periodic structure with multiple frequencies. To introduce this concept for diagonal matrices, let us consider only two different frequencies ω_1, ω_2 and without any phase factor term. In this case, the general matrix with cosines on the diagonal can be written using a weighted combination with two coefficients. More generally, if we consider a signal consisting of p cosines with different frequencies an LCU with p terms corresponds to

$$\sum_{j=0}^{p-1} \alpha_j U_{C(\omega_j)}, \tag{21}$$

with a complexity of $O(p \log N)$. This result is a generalization of the GQSP framework [19] since it can express the frequency ω not necessarily as a root of unity $2\pi/N$. We can reformulate this result including also sine waves. In particular, given a generic $T-$periodic

real function expressed as a trigonometric series with appropriate coefficients

$$f(x) = \frac{a_0}{2} + \sum_{n=1}^{\infty} \left[a_n \cos\left(\frac{2\pi}{T} n x\right) + b_n \sin\left(\frac{2\pi}{T} n x\right) \right], \tag{22}$$

it is possible to implement a block encoding of the $N \times N$ diagonal matrix $\mathcal{A}$ such that

$$\mathcal{A} |x\rangle = f(x) |x\rangle , \tag{23}$$

using an LCU employing block encodings of the *cosine* and *sine* matrix defined in Equations (2) and (3). The proposed methodology can be more efficient than the one used in GQSP which relies on a signal decomposition into a $d-$degree polynomial of $V(\omega)$ requiring $\mathcal{O}(d \log N)$ 1 and 2 qubits gates. The two methods are equivalent when ω can be written as an integer multiplied by the root of unity $2\pi/N$. However, in the more general case, the order d needed for the GQSP-based approach can be much larger than the order p required by our method. A simple example is for a matrix proportional to $C(\pi N/(N + 1))$ requiring only $p = 1$ for our method, which then costs $\mathcal{O}(\log(N))$, but for GQSP the cost becomes $\mathcal{O}(N \log(N))$ due to the need to use a $d = N$ polynomial. It remains to be explored whether this approach can be generalized using matrix access oracles [9] and whether that would result in a computational advantage. Specifically, an open research question is whether it is possible to design a oracle to pick between various frequencies, such that the final block encoded operator represents the sum of different components.

Let us now discuss the case of periodic matrices of Equation (13). Considering again only two frequencies, using four positive real coefficients for the LCU it is possible to write the overall matrix M expanded as

$$M = \alpha_0 C(\omega_1) + \alpha_1 L + \alpha_2 R + \alpha_3 C(\omega_2), \tag{24}$$

with corresponding diagonal entries

$$m_{ii} = \alpha_0 \cos((i-1)\omega_1) + \alpha_3 \cos((i-1))\omega_2), \quad i = 1, \dots, N. \tag{25}$$

In Figure 7 it is shown the additional operator required for this case, which needs to be included in the previous LCU circuit between the $PREP$ and $PREP^\dagger$ unitaries.

4 Applications

The simulation of classical systems, in the form of partial differential equations, is of major interest for many engineering and scientific applications. Investigating the potential computational advantage enabled by quantum algorithms in addressing this task is of substantial importance. In this section we apply the proposed methodology to different model problems.
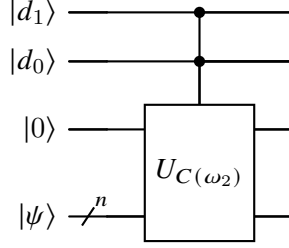
Figure 7: Controlled operation to include another frequency. An additional ancillary qubit for the block encoding of $U_{C(\omega_2)}$ is employed.

4.1 Elliptic problem with periodically varying reaction

As a first example, we consider the following one-dimensional elliptic problem with periodic boundary conditions

$$\begin{cases} -Du'' + au = f & x \in (0,1) \\ u(0) = u(1) \end{cases} \tag{26}$$

with a constant diffusion coefficient $D = 1$ and a positive periodically varying reaction term $a(x) = a_0 + \cos(\omega x)$ with $a_0 > 1$. We emphasize that the reaction term does not need to be periodic with period equal to the domain length. This formulation can be used to find the ground state of a particle in a periodic potential. For simplicity, we consider also a constant real coefficient for the source term $f = 1$. Using a centered finite difference scheme to approximate the second derivative, on a uniform discretization of spacing $h = 1/N$ inside $(0,1)$, the problem can be written as a linear system of equations of dimension N

$$A\mathbf{u} = \mathbf{f}, \tag{27}$$

where $\mathbf{u} = (u_1, u_2, \cdots, u_N)^T$ is the vector of unknowns, $\mathbf{f} = (1, 1, \cdots, 1)^T$ is the right-hand side vector, and A is the tridiagonal banded matrix

$$A = 1/h^2 \begin{bmatrix} 2 + a_1 h^2 & -1 & 0 & \cdots & & -1 \\ -1 & 2 + a_2 h^2 & \ddots & \ddots & & 0 \\ 0 & -1 & \ddots & -1 & & \vdots \\ \vdots & & \ddots & \ddots & \ddots & -1 \\ -1 & 0 & & \cdots & -1 & 2 + a_N h^2 \end{bmatrix}. \tag{28}$$

We use the notation $u_j = u(x_j), a_j = a(x_j)$ for the nodes $x_j = jh - h$, with $j = 1, 2, \ldots, N$ and the fact that $u(x_1) = u(x_{N+1})$. This symmetric matrix can be block encoded using the circuit of Figure 6 and a negative sign to the left and right shift permutation matrices. It is possible to solve this system by employing the QSVT algorithm for matrix inversion[28]. More in detail, QSVT requires access to the block encoding of the linear

system matrix and to prepare an initial state proportional to $\mathbf{f}$. The application of the matrix A^{-1} is achieved through a spectral transformation to the singular values of A using a polynomial approximation of the function $f(x) = \frac{1}{x}$.

4.2 ADR system with periodically varying reaction term

We consider here a prototypical case being the advection-diffusion-reaction system and discuss the feasibility of a quantum simulation method applying the proposed block encoding scheme. The ADR model can be used, for instance, in morphogenesis to describe how biological forms, patterns, and tissue shapes arise through the interaction of chemical signaling (reaction), molecular spreading (diffusion), and transport by fluid flow (advection) [29, 30, 31].

We simplify our discussion to a one-dimensional setting of length L, and define the problem as

$$\begin{cases} \dfrac{\partial \psi}{\partial t} = \dfrac{\partial}{\partial x}\left(D\dfrac{\partial \psi}{\partial x}\right) - \dfrac{\partial (c\psi)}{\partial x} - a\psi & x \in (0, L), t > 0 \\ \psi(x, 0) = g(x) & x \in (0, L) \\ \psi(0, t) = \psi(L, t) & t > 0 \end{cases} \tag{29}$$

where $\psi(x, t)$ is the unknown scalar function with initial condition $\psi(x, 0) = g(x)$ and periodic boundary conditions are set. We consider a constant diffusion coefficient $D \in \mathbb{R}^+$, a constant velocity coefficient $c \in \mathbb{R}$ and $a : (0, L) \to \mathbb{R}^+$, $a(x) = a_0 + \cos(\omega x)$ is a positive reaction coefficient with a periodic component oscillating with (spatial) period $2\pi/\omega$. This is an extension of the analysis provided in [32], which considered only constant coefficients. This model can also be used for the Fokker-Planck equation, where the statistical distribution of particle velocities evolves under the combined effects of drag and Brownian diffusion [33]. In addition, if one sets $c = 0$ and uses quantum imaginary time evolution [34], this equation describes the unitary dynamics of a wave-packet in a one-dimensional domain under the influence of an external periodic potential.

Employing a centered finite difference scheme to approximate the derivatives with respect to the variable x on a uniform distribution of N spatial nodes the problem can be written in an algebraic form as follows

$$\begin{cases} \dfrac{d\boldsymbol{\psi}(t)}{dt} = M\boldsymbol{\psi}(t), \quad t > 0 \\ \boldsymbol{\psi}(0) = \mathbf{g}(x) \end{cases} \tag{30}$$

where the matrix M is a banded matrix with a periodic structure on the main diagonal

$$
M_{ij} = \begin{cases} -\dfrac{2D}{\Delta x^2} - a_0 - \cos(\omega x_i) & \text{if } j = i \\[2ex] \dfrac{D}{\Delta x^2} - \dfrac{c}{2\Delta x} & \text{if } (j = i+1) \text{ or } (i = N \text{ and } j = 1) \\[2ex] \dfrac{D}{\Delta x^2} + \dfrac{c}{2\Delta x} & \text{if } (j = i-1) \text{ or } (i = 1 \text{ and } j = N) \\[2ex] 0 & \text{otherwise.} \end{cases} \tag{31}
$$

It is possible to apply the forward Euler method to numerically solve (30) and obtain

$$
\begin{cases} \psi(t + \Delta t) = (I + \Delta t M)\psi(t) = A\psi(t) \\ \psi(0) = \mathbf{g}(x) \end{cases} \tag{32}
$$

where here the matrix A is, again, a banded matrix with a periodic structure on the main diagonal. In order to guarantee stability of the Forward Euler scheme, the time step Δt must satisfy a CFL condition depending on the diffusion, advection, and reaction coefficients. Both the matrix M and A can be decomposed as in equation (18).

4.3 ADR system with periodically varying velocity

As a final case we model again the ADR problem (29) in the one-dimensional domain but now with a periodically varying velocity $c = \sin(\omega x)$ term and constant diffusion and reaction terms $D, a \in \mathbb{R}^+$. In this setting the advection term can be written as

$$
\frac{\partial(c\psi)}{\partial x} = \frac{\partial c}{\partial x}\psi + c\frac{\partial \psi}{\partial x} = \omega \cos(\omega x)\psi + \sin(\omega x)\frac{\partial \psi}{\partial x}. \tag{33}
$$

Therefore, the *effective* reaction term is $a + \omega \cos(\omega x)$ which can be treated as in the previous case. By applying again a centered finite difference scheme and the forward Euler method as in (32), the resulting matrix A is

$$
A_{ij} = \begin{cases} -\dfrac{2D}{\Delta x^2} - a + \omega \cos(\omega x_i) & \text{if } j = i \\[2ex] \dfrac{D}{\Delta x^2} - \dfrac{\sin(\omega x_i)}{2\Delta x} & \text{if } (j = i+1) \text{ or } (i = N \text{ and } j = 1) \\[2ex] \dfrac{D}{\Delta x^2} + \dfrac{\sin(\omega x_i)}{2\Delta x} & \text{if } (j = i-1) \text{ or } (i = 1 \text{ and } j = N) \\[2ex] 0 & \text{otherwise,} \end{cases} \tag{34}
$$

and can be written as an LCU

$$
A = \alpha_0 C(\omega) + \alpha_1 L + \alpha_2 LS(\omega) + \alpha_3 R + \alpha_4(-RS(\omega)) + \alpha_5(-I), \tag{35}
$$

where the coefficients $\{\alpha\}_{j=0}^5$ are real numbers depending on the specific values of D and a.

5   Numerical simulations

In this section we present numerical results for the proposed methodology and the previously mentioned applications. Given the periodic matrix $C(\omega)$ defined in Equation (2) we compared the proposed methodology to the FABLE method to analyze different block encoding strategies. As shown in Figure 8, the block encoding of this work $U_{C(\omega)}$ has a linear complexity compared to the more general FABLE method which scales exponentially with respect to the number of qubits n. The linear scaling is replaced for a banded matrix, defined by the LCU of Equation (18), by a either a linear or quadratic one depending on the implementation of the L and R matrices.
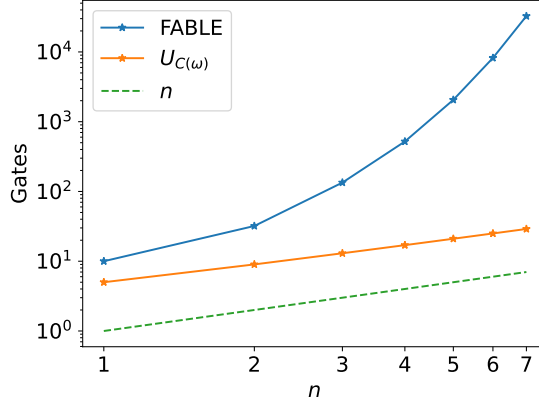

Figure 8: Number of operations with respect to the number of qubits n for the block encoding of the diagonal matrix $C(\omega)$ using the FABLE library and the block encoding scheme proposed in this work $U_{C(\omega)}$ for $\omega = 2$. The circuit are constructed with Qiskit and transpiled to a generic quantum hardware counting single and two-qubits gates. The scale is logarithmic for both axes.

We have numerically verified the proposed methodology using Qiskit and the pyqsp library to implement the QSVT algorithm. The pyqsp library serves as a computationally efficient tool to calculate the corresponding phase factors for a given polynomial transformation of the singular values of the input matrix [35]. In Figures 9 and 10 we compare the QSVT result to the ones achieved by a classical linear system solver for the problem (26) in two different settings. The first case is with $D = 1$, $\omega = 2$ and $a(x) = 1.5 + \cos(\omega x)$ in a computational grid using $N = 8$ nodes for the periodic $u(0) = u(1)$ solution, and the second case employs $D = 0.1$, $\omega = 1$. The pyqsp library has been used to find the phase factors for the polynomial approximation of $1/x$ in the interval $[1/k, 1]$ using the procedure described in [36] and $k = 3$ or 4. The second case achieves a more accurate result with QSVT since the condition number of the matrix is smaller. To achieve higher accuracy and a lower discrepancy with the classical solution, a larger value of k should be used since the condition number of the input matrix is high even for such a coarse spatial discretization.

15

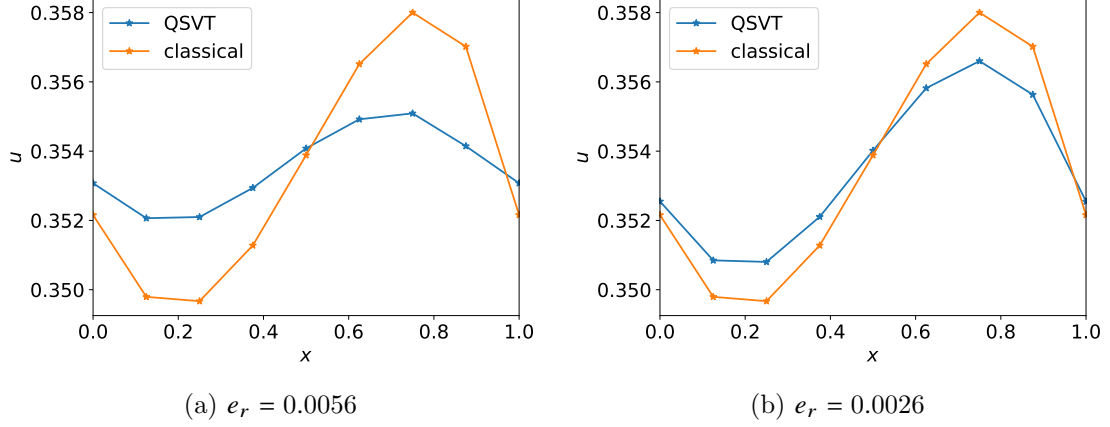(a) $e_r = 0.0056$ (b) $e_r = 0.0026$

Figure 9: Comparison between (normalized) classical result and QSVT simulation for the elliptic problem (26) with $D = 1$, $\omega = 2$ and $a(x) = 1.5 + \cos(\omega x)$ (a) for the case $k = 3$ and (b) for the case $k = 4$. For both cases the relative error in the Euclidean norm e_r has been computed.
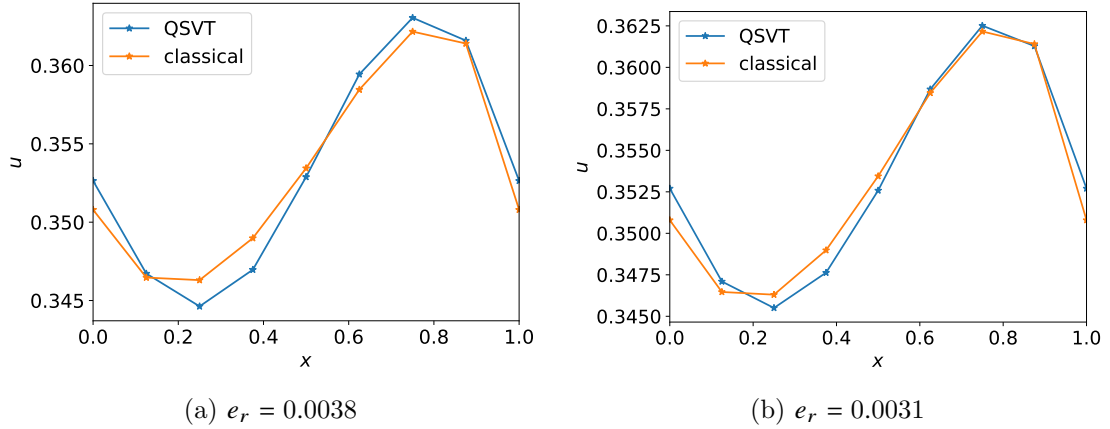

(a) $e_r = 0.0038$ (b) $e_r = 0.0031$

Figure 10: Comparison between (normalized) classical result and QSVT simulation for the elliptic problem (26) with $D = 0.1$, $\omega = 1$ and $a(x) = 1.5 + \cos(\omega x)$ (a) for the case $k = 3$ and (b) for the case $k = 4$. For both cases the relative error in the Euclidean norm e_r has been computed.

For the ADR system we employed again QSVT for the periodically varying reaction term case tackling different configurations for the reaction term. In the simulations we take $c = 0$ and a constant value of the diffusion coefficient D in order to have $D/\Delta x^2 = 0.2$. In this case the pyqsp library has been used to find the phase factors to implement, for a given simulation time t, the polynomial approximation of $f(x) = e^{xt}$ as applied to the eigenvalues of the matrix M of Equation (31). In Figure 11 the results of the simulations, for an initial Gaussian profile, are compared to the exact classical simulations computing

16

e^{Mt} for different times expressed in units of the cell diffusion time $\tau_d = \Delta x^2/D$. The state evolves accordingly to the reaction term modifying its shape with time as expected. Four cases are shown, in the upper row (a) with a reaction term of $a(x) = 0.1 + 0.01 \sin(\frac{2\pi}{16}x)$ and (b) with $a(x) = 0.1 + 0.01 \cos(\frac{2\pi}{16}x)$ (b). In the lower row (c) with reaction of $a(x) = 0.1 + 0.01 \sin(\frac{2\pi}{16}x) + \frac{0.01}{3} \sin(\frac{6\pi}{16}x)$ and (d) $a(x) = 0.1 - 0.01 \sin(\frac{2\pi}{16}x) + \frac{0.01}{9} \sin(\frac{6\pi}{16}x)$.
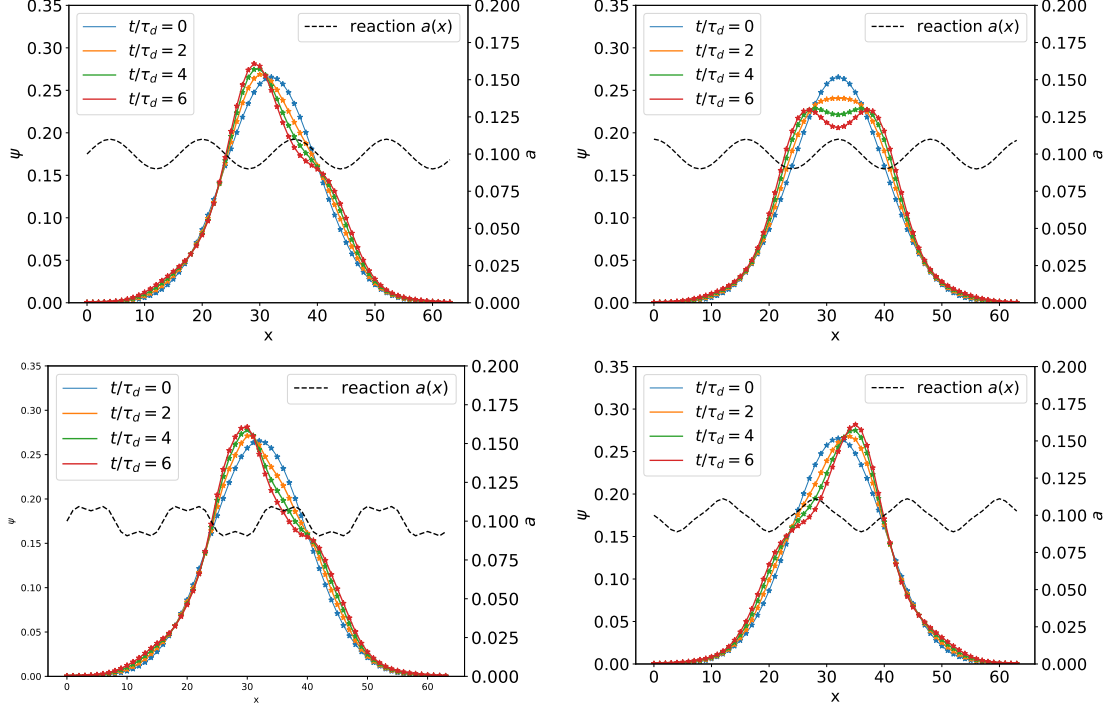

Figure 11: QSVT simulation (dots) for a periodically varying reaction term without the advection term $c = 0$ implementing a block encoding of e^{Mt} for the matrix M of Equation (31), compared with the exact result (solid line) and where the dashed lines represent the reaction term. The four cases shown are with different reaction terms: (a) sine wave, (b) cosine wave, (c) sum of two sines reproducing a square wave and (d) sum of two sines reconstructing a triangular wave.

6 Conclusion

In this work we presented a low volume (circuit depth and size) quantum circuit for block encoding sparse matrices with an inherent structure. In particular, we exploit the underlying periodicity to achieve better efficiency than general-purpose methods, a consistent finding in the block encoding research [37]. For the case of a matrix with a structure on the main diagonal the circuit achieves a gate complexity that scales linearly with the number of qubits $\mathcal{O}(n)$. The proposed methodology is also capable of handling signals consisting of different frequency components, making it versatile for a wide range

17

of applications. Our work can be considered as a generalization of the GQSP method where the frequency ω is not restricted to integer multiples of $2\pi/N$, enabling an efficient way to express generic signals [19]. The advantage of the proposed methodology compared to the existing literature lies in exploiting appropriately periodicity to reduce depth and avoid generic sparse or dense encodings. Our approach is particularly advantageous when the signal to be decomposed admits a compact Fourier representation so that only a small number of terms for the LCU is required. We have demonstrated the utility of the proposed block encoding through various use cases in simulating classical dynamics in one spatial dimension.

Despite the positive findings, several points still need to be addressed to further develop the proposed block encoding approach. For a generic signal to be encoded in a diagonal non-unitary matrix there is the possibility of a more efficient quantum circuit. While the LCU method for handling multiple frequencies requires ancilla qubits, which may limit scalability, alternative approaches may offer reduced resource overhead [38]. Moreover, the sub-normalization factor in the LCU setting, here considered, may be sub-optimal. A key open problem is the development of a more general framework for frequency selection, potentially based on matrix-access oracle models.

In summary, our work provides a practical framework for efficiently block encoding structured sparse matrices on quantum hardware, offering a starting point for simulating classical and quantum systems with inherent periodicity on quantum computers.

References

[1] Richard P Feynman. Simulating physics with computers. *International journal of theoretical physics*, 21(6/7):467–488, 1982.

[2] Ashley Montanaro. Quantum algorithms: an overview. *npj Quantum Information*, 2(1):1–8, 2016. `doi:10.1038/npjqi.2015.23`.

[3] Alberto Di Meglio et al. Quantum Computing for High-Energy Physics: State of the Art and Challenges. *PRX Quantum*, 5(3):037001, August 2024. Publisher: American Physical Society. URL: `https://link.aps.org/doi/10.1103/PRXQuantum.5.037001`, `doi:10.1103/PRXQuantum.5.037001`.

[4] Y. S. Weinstein, M. A. Pravia, E. M. Fortunato, S. Lloyd, and D. G. Cory. Implementation of the quantum fourier transform. *Phys. Rev. Lett.*, 86:1889–1891, Feb 2001. URL: `https://link.aps.org/doi/10.1103/PhysRevLett.86.1889`, `doi:10.1103/PhysRevLett.86.1889`.

[5] Guang Hao Low and Isaac L Chuang. Hamiltonian simulation by qubitization. *Quantum*, 3:163, 2019.

[6] Quynh T. Nguyen, Bobak T. Kiani, and Seth Lloyd. Block-encoding dense and full-rank kernels using hierarchical matrices: applications in quantum numerical linear algebra. *Quantum*, 6:876, December 2022. `doi:10.22331/q-2022-12-13-876`.

[7] Shantanav Chakraborty, András Gilyén, and Stacey Jeffery. The Power of Block-Encoded Matrix Powers: Improved Regression Techniques via Faster Hamiltonian Simulation. In Christel Baier, Ioannis Chatzigiannakis, Paola Flocchini, and Stefano Leonardi, editors, *46th International Colloquium on Automata, Languages, and Programming (ICALP 2019)*, volume 132 of *Leibniz International Proceedings in Informatics (LIPIcs)*, pages 33:1–33:14, Dagstuhl, Germany, 2019. Schloss Dagstuhl – Leibniz-Zentrum für Informatik. URL: https://drops.dagstuhl.de/entities/document/10.4230/LIPIcs.ICALP.2019.33, doi:10.4230/LIPIcs.ICALP.2019.33.

[8] Joran van Apeldoorn and András Gilyén. Improvements in Quantum SDP-Solving with Applications. In Christel Baier, Ioannis Chatzigiannakis, Paola Flocchini, and Stefano Leonardi, editors, *46th International Colloquium on Automata, Languages, and Programming (ICALP 2019)*, volume 132 of *Leibniz International Proceedings in Informatics (LIPIcs)*, pages 99:1–99:15, Dagstuhl, Germany, 2019. Schloss Dagstuhl – Leibniz-Zentrum für Informatik. URL: https://drops.dagstuhl.de/entities/document/10.4230/LIPIcs.ICALP.2019.99, doi:10.4230/LIPIcs.ICALP.2019.99.

[9] Daan Camps, Lin Lin, Roel Van Beeumen, and Chao Yang. Explicit quantum circuits for block encodings of certain sparse matrices. *SIAM Journal on Matrix Analysis and Applications*, 45(1):801–827, 2024. doi:10.1137/22M1484298.

[10] Daan Camps and Roel Van Beeumen. Fable: Fast approximate quantum circuits for block-encodings. In *2022 IEEE International Conference on Quantum Computing and Engineering (QCE)*, pages 104–113. IEEE, 2022.

[11] B David Clader, Alexander M Dalzell, Nikitas Stamatopoulos, Grant Salton, Mario Berta, and William J Zeng. Quantum resources required to block-encode a matrix of classical data. *IEEE Transactions on Quantum Engineering*, 3:1–23, 2023.

[12] Abhishek Setty. Block encoding of sparse matrices via coherent permutation. *arXiv preprint arXiv:2508.21667*, 2025.

[13] Vittorio Giovannetti, Seth Lloyd, and Lorenzo Maccone. Quantum random access memory. *Phys. Rev. Lett.*, 100:160501, Apr 2008. URL: https://link.aps.org/doi/10.1103/PhysRevLett.100.160501, doi:10.1103/PhysRevLett.100.160501.

[14] Daan Camps and Roel Van Beeumen. Fable: Fast approximate quantum circuits for block-encodings. In *2022 IEEE International Conference on Quantum Computing and Engineering (QCE)*, pages 104–113, 2022. doi:10.1109/QCE53715.2022.00029.

[15] Parker Kuklinski and Benjamin Rempfer. S-fable and ls-fable: Fast approximate block-encoding algorithms for unstructured sparse matrices. *arXiv preprint arXiv:2401.04234*, 2024.

[16] William A. Simon, Carter M. Gustin, Kamil Serafin, Alexis Ralli, Gary R. Goldstein, and Peter J. Love. Ladder Operator Block-Encoding. *Quantum*, 9:1953, December 2025. `doi:10.22331/q-2025-12-22-1953`.

[17] Michael A. Nielsen and Isaac L. Chuang. *Quantum Computation and Quantum Information: 10th Anniversary Edition.* Cambridge University Press, 2010. `doi:10.1017/CBO9780511976667`.

[18] Yunseong Nam, Yuan Su, and Dmitri Maslov. Approximate quantum Fourier transform with O(n log(n)) T gates. *npj Quantum Information*, 6(1):26, March 2020. `doi:10.1038/s41534-020-0257-5`.

[19] Danial Motlagh and Nathan Wiebe. Generalized quantum signal processing. *PRX Quantum*, 5:020368, Jun 2024. URL: `https://link.aps.org/doi/10.1103/PRXQuantum.5.020368`, `doi:10.1103/PRXQuantum.5.020368`.

[20] Julien Zylberman, Ugo Nzongani, Andrea Simonetto, and Fabrice Debbasch. Efficient quantum circuits for non-unitary and unitary diagonal operators with space-time-accuracy trade-offs. *ACM Transactions on Quantum Computing*, 6(2), April 2025. `doi:10.1145/3718348`.

[21] Adriano Barenco, Charles H. Bennett, Richard Cleve, David P. DiVincenzo, Norman Margolus, Peter Shor, Tycho Sleator, John A. Smolin, and Harald Weinfurter. Elementary gates for quantum computation. *Phys. Rev. A*, 52:3457–3467, Nov 1995. URL: `https://link.aps.org/doi/10.1103/PhysRevA.52.3457`, `doi:10.1103/PhysRevA.52.3457`.

[22] Ben Zindorf and Sougato Bose. Efficient Implementation of Multi-Controlled Quantum Gates, March 2025. arXiv:2404.02279 [quant-ph]. URL: `http://arxiv.org/abs/2404.02279`, `doi:10.48550/arXiv.2404.02279`.

[23] Craig Gidney. Halving the cost of quantum addition. *Quantum*, 2:74, June 2018. `doi:10.22331/q-2018-06-18-74`.

[24] Randall J. LeVeque. *Finite Difference Methods for Ordinary and Partial Differential Equations.* Society for Industrial and Applied Mathematics, 2007. URL: `https://epubs.siam.org/doi/abs/10.1137/1.9780898717839`, `arXiv:https://epubs.siam.org/doi/pdf/10.1137/1.9780898717839`, `doi:10.1137/1.9780898717839`.

[25] Alfio Quarteroni, Riccardo Sacco, and Fausto Saleri. *Numerical mathematics*, volume 37. Springer Science & Business Media, 2010. `doi:10.1007/978-0-387-22750-4`.

[26] Andrew M. Childs and Nathan Wiebe. Hamiltonian simulation using linear combinations of unitary operations. *Quantum Info. Comput.*, 12(11–12):901–924, November 2012.

[27] Ryan Babbush, Craig Gidney, Dominic W. Berry, Nathan Wiebe, Jarrod McClean, Alexandru Paler, Austin Fowler, and Hartmut Neven. Encoding electronic spectra in quantum circuits with linear t complexity. *Phys. Rev. X*, 8:041015, Oct 2018. URL: https://link.aps.org/doi/10.1103/PhysRevX.8.041015, doi:10.1103/PhysRevX.8.041015.

[28] John M. Martyn, Zane M. Rossi, Andrew K. Tan, and Isaac L. Chuang. Grand Unification of Quantum Algorithms. *PRX Quantum*, 2(4):040203, December 2021. URL: https://link.aps.org/doi/10.1103/PRXQuantum.2.040203, doi:10.1103/PRXQuantum.2.040203.

[29] Sauro Succi. *The Lattice Boltzmann Equation for Fluid Dynamics and Beyond*. Oxford University Press, 06 2001. doi:10.1093/oso/9780198503989.001.0001.

[30] S. G. Ayodele, F. Varnik, and D. Raabe. Lattice boltzmann study of pattern formation in reaction-diffusion systems. *Phys. Rev. E*, 83:016702, Jan 2011. URL: https://link.aps.org/doi/10.1103/PhysRevE.83.016702, doi:10.1103/PhysRevE.83.016702.

[31] Thiparat Chotibut, David R. Nelson, and Sauro Succi. Striated populations in disordered environments with advection. *Physica A: Statistical Mechanics and its Applications*, 465:500–514, 2017. URL: https://www.sciencedirect.com/science/article/pii/S0378437116305830, doi:10.1016/j.physa.2016.08.059.

[32] Claudio Sanavio, Enea Mauri, and Sauro Succi. Explicit quantum circuit for simulating the advection–diffusion–reaction dynamics. *IEEE Transactions on Quantum Engineering*, 6:1–12, 2025. doi:10.1109/TQE.2025.3544839.

[33] Hannes Risken. Fokker-planck equation. In *The Fokker-Planck equation: methods of solution and applications*, pages 63–95. Springer, 1989.

[34] Mario Motta, Chong Sun, Adrian TK Tan, Matthew J O'Rourke, Erika Ye, Austin J Minnich, Fernando GSL Brandao, and Garnet Kin-Lic Chan. Determining eigenstates and thermal states on a quantum computer using quantum imaginary time evolution. *Nature Physics*, 16(2):205–210, 2020. doi:10.1038/s41567-019-0704-4.

[35] Yulong Dong, Xiang Meng, K. Birgitta Whaley, and Lin Lin. Efficient phase-factor evaluation in quantum signal processing. *Phys. Rev. A*, 103:042419, Apr 2021. URL: https://link.aps.org/doi/10.1103/PhysRevA.103.042419, doi:10.1103/PhysRevA.103.042419.

[36] Andrew M Childs, Robin Kothari, and Rolando D Somma. Quantum algorithm for systems of linear equations with exponentially improved dependence on precision. *SIAM Journal on Computing*, 46(6):1920–1950, 2017.

[37] Parker Kuklinski, Benjamin Rempfer, Justin Elenewski, and Kevin M. Obenland. Efficient block-encodings require structure. 2025. URL: https://api.semanticscholar.org/CorpusID:281505340.

[38] Francisca Vasconcelos and András Gilyén. Methods for reducing ancilla-overhead in block encodings, 2025. URL: https://arxiv.org/abs/2507.07900, arXiv:2507.07900.

MOX Technical Reports, last issues

Dipartimento di Matematica

Politecnico di Milano, Via Bonardi 9 - 20133 Milano (Italy)

14/2026   Agasisti, T.; Cannistrà, M.; Paganoni, A.M.
Nudging communication for students at risk: experimental evidence from an Italian university

13/2026   Dimola, N.; Coclite, A.; Zunino, P.
Neural Preconditioning via Krylov Subspace Geometry

12/2026   Corbetta A; Logan K.M.; Ferro M; Zuccolo L; Perola M.; Ganna A.; Di Angelantionio E.;Ieva F.
Longitudinal patterns of statin adherence and factors associated with decline in over one million individuals in Finland and Italy

11/2026   Cicalese, G.; Ciaramella, G.; Mazzieri, I.; Gander, M. J.
Optimized Schwarz Waveform Relaxation for the Damped Wave Equation

10/2026   Dimola, N.; Franco, N. R.; Zunino, P.
Numerical Solution of Mixed-Dimensional PDEs Using a Neural Preconditioner

09/2026   Manzoni, V.; Ieva, F.;Larranaga, A.C.; Vetrano, D.L.; Gregorio, C.
Hidden multistate models to study multimorbidity trajectories

08/2026   Micheletti, S.
Newmark time marching as a preconditioned iteration for large SPD linear systems

Micheletti, S.
Newmark time marching as a preconditioned iteration for large SPD linear systems

07/2026   Corti, M.; Ahern, A.; Goriely, A.; Kuhl, E.; Antonietti, P.F.
A whole-brain model of amyloid beta accumulation and cerebral hypoperfusion in Alzheimer's disease

05/2026   Ranno, A.; Ballarin, F.; Lespagnol, F.; Zunino, P.; Perotto, S.
A fictitious domain formulation based on hierarchical model reduction applied to drug-eluting stents